Control Oriented Tire and Chassis Model for Low Velocities on Uneven Roads

Authors: Fabian Walz[1], Binjun Lu[1], Prof. Dr.-Ing. Sören Hohmann[2]
Institutions: [1]Daimler AG, Böblingen, Germany
[2]Institute for Control Systems, Karlsruhe Institute of Technology, Germany
Contact: fabian.walz@daimler.com

Abstract: *In this paper we investigate the dynamics of tires and suspension which are relevant for vehicle longitudinal motion control at low velocities in case of uneven road surfaces or obstacles on the road. We use a simplified version of the Radial Spring Model and extend it to cover rotational dynamics without using an additional enveloping model. We use a simple bicycle model for chassis dynamics. For the use case of driving up and down a stepped obstacle we present real world measurements including spindle torque and forces of the wheels. The aim of this paper is to present a simple model that shows a good fit with measurement data for step sizes up to 14 cm. To prevent small model inaccuracies of yielding significant differences between measured and simulated behavior, we propose a controller to replicate the measured wheel motion. The simulated spindle torque and forces are compared to the measurements and to the well known Tandem Elliptical Cams enveloping model. The key findings of our work include that our model represents the fundamental dynamics of the scenario quite well. For high step sizes the proposed model yields significantly better results than the enveloping model.*

Keywords: Tire Model, Point Contact Model, Two Point Model, Tandem Ellipctical Cams, Chassis Model, Step Driving, Wheel Force Sensor, Measurment Rims, Real World Measurements, Model Validation, Longitudinal Control, Systems Theory, Cybernetics

I. Introduction

A. Motivation

Vehicle longitudinal motion control is a fundamental technology in modern road vehicles and has therefore already been subject to research for a couple of decades. Up to now however, research on longitudinal control design has focused on achieving adequate performance in the most common and benign conditions [12]. With automated driving of the SEA levels 4 and 5 [1] new challenges arise, since the number of use cases and thus the broadness of the operating range increases. Obviously, there will be no human driver as backup system. In order to develop efficient and reliable control systems we need to work out the worst case scenarios for longitudinal control. At low vehicle speeds, disturbances are to a great extent excited by the road surface and obstacles. It therefore seems natural to investigate the impacts of these disturbances and how to make longitudinal control more robust towards them.

During the normal, everyday use of a car, it encounters excitation through road surface in various manners. Especially while parking and making turns, driving over bumps and curbs is quite common. Speed bumps and potholes are found on an increasing number of roads. Some countries use pits to separate road and pedestrian walkways that need to be passed while turning. In all of those cases, approaching the obstacle with sufficient speed will result in overrunning it without much influence on the vehicles longitudinal motion. Driving slowly or coming to a stop and then moving on again in immediate proximity of such an obstacle, however, proves to be a very difficult task due to limitations of vehicle sensors and actuators.

Figure 1: *Vehicle with all wheel drive standing in front of a curb.*

Consider a vehicle standing with one axle right in front of a step like in figure 1. This means that there is a significant amount of torque necessary to overcome this disturbance and get the vehicle climb up the obstacle. However, the disturbance vanishes immediately after the climb and the vehicle will accelerate if the drive torque is not reduced fast enough. In

practice we experienced that the use of standard linear control designs like PID results in getting stuck or overshooting the set values for acceleration, velocity and driven distance significantly. This not only poses impairments of driving comfort but also a serious safety hazard.

Beyond the scope of these standard use cases emerge additional and even more challenging scenarios if we look at possible applications in the automotive production process. For automated vehicle testing the longitudinal control must be able to roll on and of dynamometers and perform on difficult ground like cobblestone and terrain. If a car shall be able to drive itself all the way from the end of the production line to shipping it must be able to drive onto car transporters and car-carrying trains.

An obvious way to approaching these challenges is the use of model based control. One therefore faces two challenges:

1. A simple yet precise model of these scenarios and their influences on longitudinal motion is needed for simulation and control synthesis.

2. Suitable controller and if necessary observer techniques must be investigated.

In this work we address the first of these challenges.

B. Previous Work

The tire model is arguably a crucial aspect in modeling the longitudinal dynamics at low speeds, since the tire effectively filters the road profile and therefore defines spindle forces and torque. A good comparison of different types of analytical tire models can be found in [22]. Some models only reproduce vertical dynamics (i.e. Footprint Model), while others also aim on covering the comfort relevant high frequency domain and thus become elaborate (i.e. Flexible Ring Model).

Although there is no lack of tire models in the literature, modeling the contact between tires and large obstacles like curbstones is only occasionally found. Most publications on this topic focus on the simulation of vehicle durability and rollover behavior in the high speed and high frequency domain. Thus, they rely on multi body or finite element approaches [10, 11, 16, 17] which are hardly suitable for online simulation, observation and control design. Other authors [4, 8, 13] use simpler approaches with varying aspects of the Radial Spring or Flexible Ring Model [6, 7, 22] but without application to control of real world systems. Many of these publications do not consider the rotatory freedom of the tire and therefor do not investigate the modeling of the tangential forces. Classically, control system design has been done using much simpler models [15].

Map-type or Pacejka-type models [18] that are generally used for control design do not apply in our case because they are usually designed to work on a plane road. There exist well known enveloping models as extensions. The Tandem Model with Elliptical Cams [19] calculates an equivalent ground plane that can be used instead of the actual road profile. However, such extensions work for relatively small step sizes only, as we will show in comparison.

Research on longitudinal control itself mostly focuses on evaluating various control techniques and design methods for use cases like adaptive cruise control and platooning. Using more advanced vehicle and tire models is a comparatively new area of interest. These works mainly focus on improving ride comfort [9, 14] and handling [21].

The remainder of this paper is structured as follows: In section II we will present our simulation model and deduce its equations of motion. We will briefly introduce our experimental vehicle and its measurement equipment in section III. Thereafter, we will explain how the measurement data can be used both to provide simulation input and to assess the models accuracy in section IV. We will also discuss the obtained simulation results. Finally, section V summarizes our work.

II. Modeling

In this section we will work out the equations of motion for a plane (2D) bicycle model of a vehicles longitudinal dynamics at very low speeds. The combined model will use the equations of motion of the tire model two times (front and rear wheel). It includes the tire model, the representation of the road profile and the chassis model.

A. Tire Model

Our use case concentrates on low speed driving. Vertical dynamics (driving comfort) is not our main concern. We will therefore base our model on the radial spring concept and extend it to also cover the wheels rotational degree of freedom.

Figure 2 shows our tire model for step driving. Instead of using a number of equally spaced radial springs, we use a maximum of

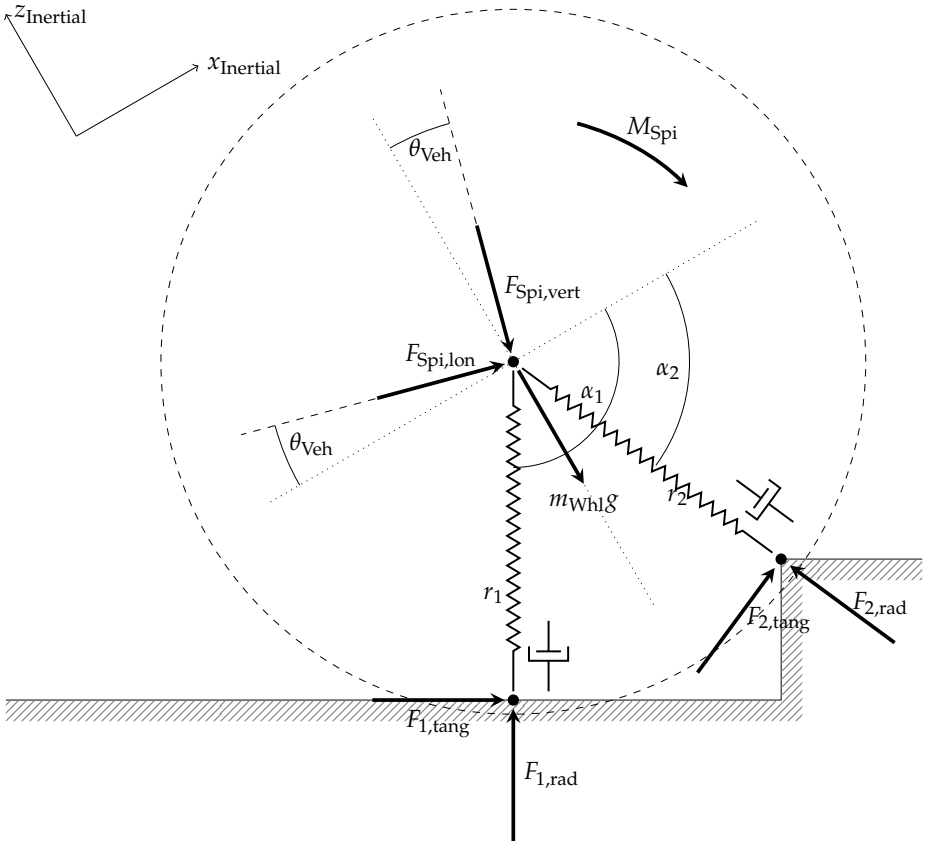

Figure 2: *Schematic representation of the two point wheel model. Depicted is the case in which the wheel rolls downhill over a curb. The damper symbols indicate the connection between wheel center and contact point by springs and dampers in parallel.*

two contact points, where one lies on the plane road and one on the edge of the step. We therefore call this specific configuration the *Two Point Model*. Both contact points are connected with the wheel center (spindle) over a spring and a damper in parallel, each. They represent separated contact zones of tire and ground. For n contact points we can derive the equations of motion of the wheel center in world coordinates as follows:

$$\ddot{x}_{\text{Spi}} m_{\text{Whl}} = \cos\theta_{\text{Veh}} F_{\text{Spi,lon}} - \sin\theta_{\text{Veh}} F_{\text{Spi,vert}} + \sum_{i=1}^{n} \sin\alpha_i F_{i,\text{tang}} - \sum_{i=1}^{n} \cos\alpha_i F_{i,\text{rad}}\,, \tag{1a}$$

$$\ddot{z}_{\text{Spi}} m_{\text{Whl}} = -\sin\theta_{\text{Veh}} F_{\text{Spi,lon}} - \cos\theta_{\text{Veh}} F_{\text{Spi,vert}} + \sum_{i=1}^{n} \cos\alpha_i F_{i,\text{tang}} + \sum_{i=1}^{n} \sin\alpha_i F_{i,\text{rad}} - m_{\text{Whl}} g\,, \tag{1b}$$

$$\ddot{\theta}_{\text{Spi}} J_{\text{Whl}} = M_{\text{Spi}} - \sum_{i=1}^{n} r_i F_{i,\text{tang}}\,. \tag{1c}$$

The spindle forces $F_{\text{Spi,lon}}$ and $F_{\text{Spi,vert}}$ are a result of the vehicles weight and motion. They are calculated together with the vehicle pitch angle θ_{Veh} in the chassis model. The spindle torque M_{Spi} is a result of the powertrain and the brakes. From the tire models point of view, these variables are considered to be inputs.

The radial forces depend on the distance between contact points and wheel center

$$F_{i,\text{rad}} = (r_0 - r_i) c_{\text{rad}} + \dot{r}_i k_{\text{rad}} \tag{2a}$$

and are constrained to non negative values

$$F_{i,\text{rad}} \geq 0\,. \tag{2b}$$

Depending on the number of springs and the arrangement of the contact points, these are also the equations of motion for the well-known Point Contact ($n = 1$) and Radial Spring Model (many, equally spaced springs).

Since we are interested in low speeds, the transient properties of the tires longitudinal dynamics are relevant. The tangential forces $F_{i,\text{tang}}$ are a result of the bristle deflection (see brush model [18]). A common slip model is the series

connection of a spring and a damper

$$\dot{F}_{i,\text{tang}} = -\frac{2}{l_{\text{cntct}}} \left| r_{\text{dyn}} \dot{\theta}_{\text{Spi}} \right| F_{i,\text{tang}} + c_{\text{tang}} (r_{\text{dyn}} \dot{\theta}_{\text{Spi}} - \dot{x}_i) \tag{3a}$$

as shown in [3]. l_{cntct} is the contact patch length and $\dot{x}_i$ is the velocity of the wheel in direction of $F_{i,\text{tang}}$. Since $F_{i,\text{rad}}$ change significantly as the points gain and lose contact, we limit the tangential forces based on the friction coefficient μ:

$$F_{i,\text{tang}} \leq \mu F_{i,\text{rad}} \,. \tag{3b}$$

A list of all parameters for the tire model can be found in table 1.

Table 1: *List of parameters for the Two Point Tire Model.*

Symbol	Unit	Description
m_{Whl}	kg	Combined mass of rim, tire and brake disc
J_{Whl}	kg*m^2	Combined inertia of rim, tire and brake disc
r_0	m	Unloaded tire radius
r_{dyn}	m	Dynamic tire radius
l_{cntct}	m	Contact patch length
μ	1	Friction coefficient
c_{rad}	N/m	Radial spring constant
k_{rad}	N*s/m	Radial damper constant
c_{tang}	N/m	Tangential spring constant

B. Chassis Model

The schematic of the chassis model can be found in figure 3. Since, in our scenario, the chassis transmits considerable forces in longitudinal direction, we included springs and dampers to model the longitudinal flexibility.

With the vehicles mass m_{Veh} and inertia J_{Veh} the equations of motion become

$$\ddot{x}_{\text{Veh}} m_{\text{Veh}} = -\cos\theta_{\text{Veh}} F_{\text{Spi,f,lon}} - \cos\theta_{\text{Veh}} F_{\text{Spi,r,lon}} + \sin\theta_{\text{Veh}} F_{\text{Spi,f,vert}} + \sin\theta_{\text{Veh}} F_{\text{Spi,r,vert}} \,, \tag{4a}$$

$$\ddot{z}_{\text{Veh}} m_{\text{Veh}} = \sin\theta_{\text{Veh}} F_{\text{Spi,f,lon}} + \sin\theta_{\text{Veh}} F_{\text{Spi,r,lon}} + \cos\theta_{\text{Veh}} F_{\text{Spi,f,vert}} + \cos\theta_{\text{Veh}} F_{\text{Spi,r,vert}} \,, \tag{4b}$$

$$\ddot{\theta}_{\text{Whl}} J_{\text{Veh}} = -d_{\text{f,lon}} F_{\text{Spi,f,vert}} + d_{\text{r,lon}} F_{\text{Spi,r,vert}} + d_{\text{f,vert}} F_{\text{Spi,f,lon}} + d_{\text{r,vert}} F_{\text{Spi,r,lon}} - M_{\text{Spi,f}} - M_{\text{Spi,r}} \,. \tag{4c}$$

The indices denote wheel positions directions of forces.

The chassis (and therefore also spindle) forces depend on the deflections and deflection rates at each wheel $p \in \{\text{f}, \text{r}\}$ and coordinate direction $q \in \{\text{lon}, \text{vert}\}$:

$$F_{\text{Spi},p,q} = (d_{p,q,0} - d_{p,q}) c_{p,q} + \dot{d}_{p,q} k_{p,q} \,. \tag{5}$$

$d_{p,q}$ and its derivative can be calculated using the spindle positions $x_{\text{Spi},p}$, $z_{\text{Spi},p}$.

C. Parametrization

We tune the spring and damper constants of the tire model manually in order to get a good fit with our measurement data. While the tire radii where measured or obtained from experiments, we estimated the weight and inertia of tire, rim and brake disc.

Regarding our use case we do usually not get even near the friction limit. The constraint (3b) is therefore only relevant if one point loses contact with the road. Arbitrarily choosing $\mu = 1$ works well. Varying μ has nearly no influence on the overall results.

The contact patch length l_{cntct} can be measured or approximated [5]. In reality, l_{cntct} will not only differ for varying contact points, but also change with the loads $F_{i,\text{rad}}$. However, it only influences the damping part of (3a) which vanishes at low rotational speeds. Since we assume $\dot{\theta}_{\text{Spi}}$ to be small especially when the tire is in contact with a step, we neglect these differences and assume l_{cntct} to be constant and equal for both contact points.

The geometric parameters of the chassis $d_{p,q,0}$ can be estimated using measured axle loads (compare section III). The spring constants $c_{p,q}$ were measured on a similar vehicle using a test bench, while we needed to guess the damper constants $k_{p,q}$.

III. Experimental Vehicle

Identification and validation of tire models in literature is mostly done by using measurement data from special flat track or drum test benches, in which a single tire is examined. This allows experiments with small obstacle sizes, only. Furthermore, these test benches are specifically designed to test purely the tire itself. Having an experiment setup that is closer to the use case of longitudinal control is standing to reason in order to test our more comprehensive model.

The experimental vehicle that we use to collect the measurement data presented in this paper is a luxury sedan with all wheel drive and

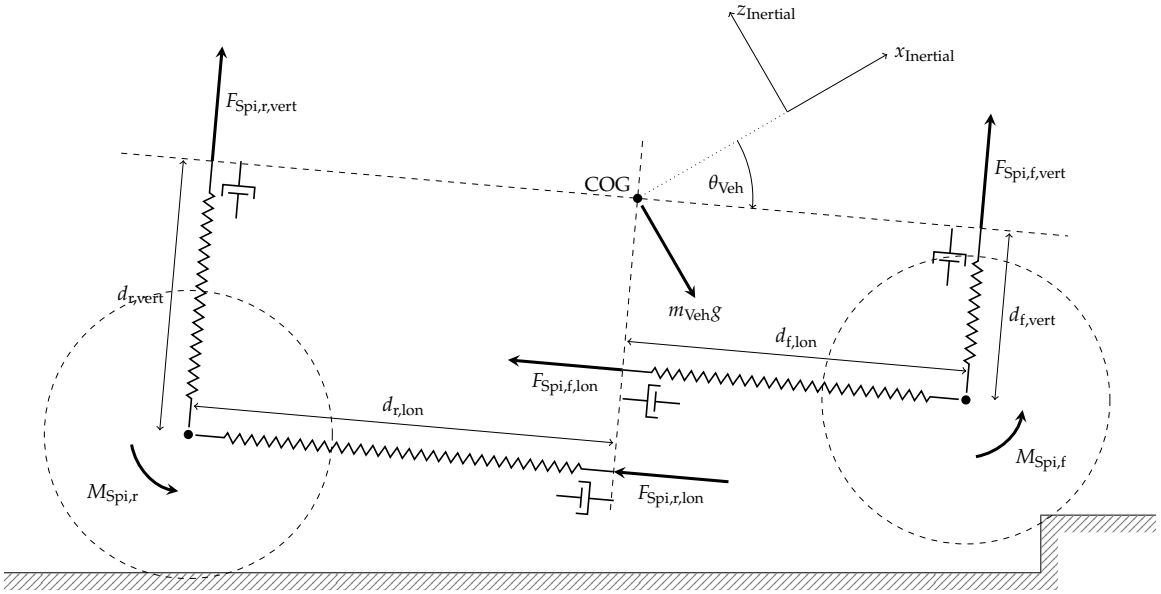

Figure 3: *Schematic representation of the chassis model. Depicted is the case in which the vehicle rolls downhill over a curb. The damper symbols indicate the connection between wheel center and contact point by springs and dampers in parallel.*

air suspension. It is equipped with four Kistler Roadyn S625 wheel force sensors [2]. These sensors measure the forces and torques between the wheel and the spindle in all three coordinate directions. In this paper however, we restrain to the two-dimensional case. A schematic drawing of such a wheel sensor is shown in figure 4.

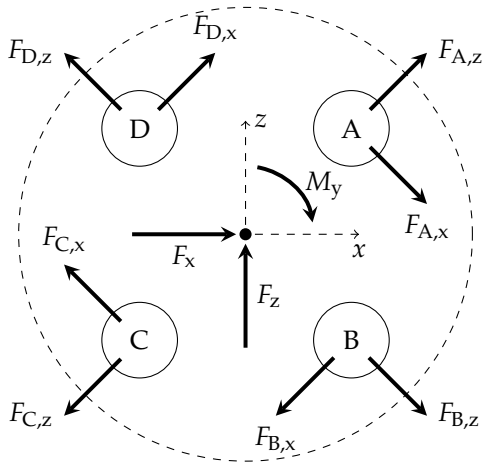

Figure 4: *Scheme of the Kistler Roadyn S625 wheel sensor and its four strain gage capsules (A, B, C and D) in the x, z plane.*

The firmware of the sensor calculates the wheel forces and torque in the vehicle coordinate system from the forces measured by four strain gage capsules. Therefore, the measurements $F_{\text{x}}, F_{\text{z}}$ and M_{y} are per definition equivalent to $F_{\text{Spi,lon}}, F_{\text{Spi,vert}}$ and M_{Spi}, except for their signs.

While M_{y} is independent of the rotation between wheel and vehicle coordinate system, F_{x} and F_{z} are not. In order to transform the coordinates accordingly, the sensor also measures the wheel angle θ_{Spi} in steps of one degree. This means that F_{x} has an uncertainty of up to $\sin(1^\circ)F_{\text{z}} \approx 100$ N in our case.

IV. Simulation

A. Scenario and Simulation Input

In this paper we investigate the scenario of driving up and down a step with the presented bicycle model as illustrated in figure 3. We conducted multiple real world measurements with step heights of 4, 11 and 14 cm, where we approached the obstacle perpendicularly such that both tires of the regarding axle touched it at the same time.

While in the simulation we assume the obstacle to have a sharp, rectangular edge and

a vertical flank, the curbs in reality had somewhat rounded edges. From multi body simulations with FTire [20], which are not part of this publication, we concluded that there are practically no differences between sharp and rounded edges regarding spindle forces and torque.

The inputs for our model are the spindle (drive / brake) torques at the wheels. Using the measured torques as inputs and comparing spindle forces and wheel rotation for evaluation may be the most straight forward way. However, driving up steps involves a bifurcation: The wheel starts moving once the drive torque is sufficiently high, otherwise the vehicle will not move up the step at all. Thus, even the slightest model inaccuracy causes significant differences between simulated and real vehicle behavior.

This issue can be avoided by controlling the wheels rotation in the simulation, as shown in figure 5. Using the measured wheel rotation as setpoint, the controller calculates the necessary wheel torque to reproduce wheel and vehicle motion. In this case we can use the differences in wheel torque and spindle forces to assess the models accuracy.

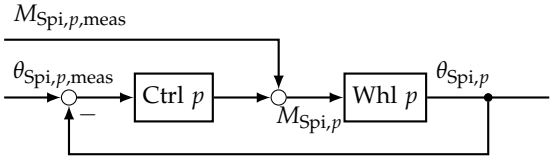

Figure 5: *Simplified block diagram of the closed control loop for wheel p in simulation.*

In detail, we use feed forward control based on the measured spindle torque $M_{\mathrm{Spi},p,\mathrm{meas}}$ and cascaded PI feedback controllers to control $\theta_{\mathrm{Spi},p}$, $\dot{\theta}_{\mathrm{Spi},p}$ and $\ddot{\theta}_{\mathrm{Spi},p}$. Therefore, the controllers output can directly be interpreted as model error. This, by implication, means that the model error we will be assessing also depends on the parametrization of the controller.

It is important to note that this control concept is only intended for simulation and will not yield satisfying results as longitudinal control concept in reality. This is mainly due to three facts:

1. The main input comes from feed forward control. The reactive feedback part only corrects for model errors.

2. There is no actuation time delay or other powertrain related effects.

3. The wheel movement $\theta_{\mathrm{Spi},p}$ and its derivatives are known with arbitrary precision.

An alternative option that avoids using feedback control is to calculate M_{Spi} from (1c). This, however, requires to differentiate $\theta_{\mathrm{Spi},p,\mathrm{meas}}$ two times, which proved to yield worse results than the controller approach.

B. Model Accuracy Estimation

In order to get an idea of the significance of errors in spindle torque, we utilize the very simple concept of a weightless rigid wheel rolling over a step, as depicted in figure 6.

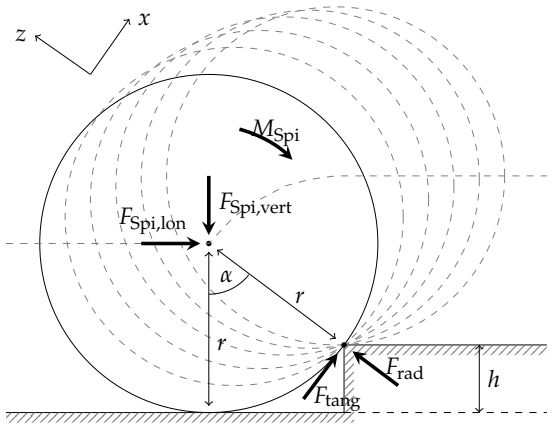

Figure 6: *Rigid wheel rolling over a step. The symbols will only become relevant in section IV.*

Let's assume we regard the front wheel of the car. The equations of motion can easily be obtained from the figure. Together with the rolling condition this leads to the force equilibrium conditions

$$M_{\mathrm{Spi}} = rF_{\mathrm{tang}}\,, \tag{6a}$$

$$0 = \cos\alpha F_{\mathrm{Spi,lon}} - \sin\alpha F_{\mathrm{Spi,vert}} + \frac{M_{\mathrm{Spi}}}{r}\,. \tag{6b}$$

From that we can calculate the sensitivities of the drive torques $\frac{\partial}{\partial h} M_{\mathrm{Spi}}$ (front driven) and $\frac{\partial}{\partial h} F_{\mathrm{Spi,lon}}$ (rear driven) with respect to the step height. Reversely, this gives us a rough but vivid estimate for what an deviation in force or torque could mean in step height. It also enables comparison with accuracy information on map data or environment scanning sensors like camera or lidar. This estimate is completely independent of the used tire model as long as spindle forces and torque are defined equivalently.[1]

[1] From this calculation we can also learn that, with increasing step height, the position of the driven axle (front or rear) gets more relevant and the difference of necessary drive torques between the two axles increases.

C. Results

Figure 7 shows the simulation and measurement of spindle torque and forces, as well as wheel rotational movement for driving up a step of 14 cm in height. The scenario matches the illustration in figure 1. It comes to no surprise that balancing the wheel on the curbs edge is a very challenging task for a human driver. Instead, the driver increases the engine torque until the vehicle moves up the step and idles the engine or brakes to move on slowly. Figure 8 shows the same graph for driving back down the step.

Our simulation model matches the measurements reasonable well. However, there are two effects related to our simulation method with feedback control, which we want to point out. The corresponding spots in the graphs are marked with arrows and the respecting number.

1. Small errors in modeling the rotational dynamics of the tires yield increasing differences in wheel rotation between simulation and measurement. Since we use feedback control to ensure equal movement, the error becomes visible in the spindle torque.

2. In some cases the closed loop tends to oscillate since we spared a damping part in the controller.

We conducted several measurements driving up and down a step with the front axle. Figures 9 and 10 show the resulting mean errors of the corresponding simulations with the chassis model and two different tire models: The proposed Two Point Model and the Point Contact model with Tandem Elliptical Cams [19]. In the legend, the mean error in torque is also expressed as an error in step height, like discussed in the previous section.

The plots show that both models fit the measurement data well for the 4 cm step. However, the accuracy of the extended Point Contact model decreases rapidly with increasing step height, while the Two Point Models accuracy stays consistently high.

V. Summary

The work presented in this paper is an elementary step on the way to accurate longitudinal motion control, when dealing with large obstacles. We introduced a combined model for tire, obstacle and chassis. Our tire model calculates tangential forces for different contact points individually and does not rely on an equivalent ground plane approach. Instead of using somewhat artificial test bench data, we showed how wheel force sensor data from a real vehicle can be used as simulation input and reference. We used a simple controller in the simulation to deal with small model inaccuracies that would otherwise render comparison with measurement data very difficult. For evaluating the models accuracy we proposed a way to estimate the practical severity of inaccuracies.

In mean, our model shows an error represented in step height of well below one centimeter. In opposition to the extended point contact model, the results are consistent for a large range of step heights. We conclude that our model covers the fundamental dynamics of the scenario and we are confident that its accuracy is sufficient for a model based longitudinal control algorithm.

Our next steps include extending and validating the model for cleats and arbitrary road profiles. It is also desirable to test the model with different types of tires and suspension systems. Our premise of approaching the obstacle with both tires perpendicularly may hold for some use cases like driving onto car transporters. The use case of urban driving (and parking), however, will likely require an extension to a two track model.

Acknowledgments

We would like to give thanks to Professor Dr. Dieter Ammon, Dr. Klaus-Peter Kuhn and Thorsten Lajewski, M.Sc. for the lively discussions about our work and their active support.

References

[1] Taxonomy and Definitions for Terms Related to Driving Automation Systems for On-Road Motor Vehicles. SAE International Standard J3016, SAE International, 2016.

[2] Kistler Instrumente AG. *Betriebsanleitung RoaDyn für System 2000*.

[3] Dieter Ammon. *Modellbildung und Systementwicklung in der Fahrzeugdynamik*. B. G. Teubner, 1997.

[4] J. M. Badalamenti and G. R. Doyle. Radial-Interradial Spring Tire Models. *Journal of Vibration, Acoustics, Stress, and Reliability in Design*, 110:70–75, January 1988.

[5] Igo Besselink. Tyre modelling. CISM Course on Vehicle Dynamics of Modern Passenger Cars, August 2016.

[6] K. M. Captain, A. B. Boghani, and D. N. Wormley. Analytical Tire Models for Dynamic Vehicle Simulation. *Vehicle System Dynamics*, 8(1):1–32, March 1979.

[7] Denny C. Davis. A Radial-Spring Terrain-Enveloping Tire Model. *Vehicle System Dynamics*, 4(1):55–69, March 1975.

[8] Terry D. Day. Simulation of Tire Interaction with Curbs and Irregular Terrain. *Washington, DC: Engineering Dynamics Corporation*, 2005.

[9] Khalid El Majdoub, Fouad Giri, Hamid Ouadi, Luc Dugard, and Fatima Zara Chaoui. Vehicle Longitudinal Motion Modeling for Nonlinear Control. *Control Engineering Practice*, 20(1):69 – 81, 2012.

[10] T. Fukashima, Hitoshi Shimonishi, Kimihiro Hayashi, and Masaki Shiraishi. Simulation of a vehicle running on to a curb by using tire and vehicle FE models. In *Proceedings of the 4th European LS-Dyna Users conference, Detroid*, 1998.

[11] V. Harth, M. Fayet, L. Maiffredy, and C. Renou. A Modelling Approach to Tire-Obstacle Interaction. *Multibody System Dynamics*, 11(1):23–39, February 2004.

[12] Jihua Huang. Vehicle Longitudinal Control. In *Handbook of Intelligent Vehicles*, pages 167–190. Springer Nature, 2012.

[13] Seongho Kim, Parviz E. Nikravesh, and Gwanghun Gim. A two-dimensional tire model on uneven roads for vehicle dynamic simulation. *Vehicle System Dynamics*, 46(10):913–930, October 2008.

[14] Shiang-Lung Koo, Han-Shue Tan, and Masayoshi Tomizuka. Impact of Tire Compliance Behavior to Vehicle Longitudinal Dynamics and Control. In *American Control Conference, 2007. ACC'07*, pages 5736–5741. IEEE, 2007.

[15] G. Leister. The role of tyre simulation in chassis development: challenge and opportunity. In *International Tyre Colloquium, 4th, 2015, Guildford, United Kingdom*, 2015.

[16] C. W. Mousseau and S. K. Clark. An Analytical and Experimental Study of a Tire Rolling Over a Stepped Obstacle at Low Velocity. *Tire Science and Technology*, 22(3):162–181, July 1994.

[17] C. W. Mousseau and G. M. Hulbert. An efficient tire model for the analysis of spindle forces produced by a tire impacting large obstacles. *Computer Methods in Applied Mechanics and Engineering*, 135(1):15–34, August 1996.

[18] Hans Pacejka. *Tire and Vehicle Dynamics*. Elsevier LTD, Oxford, 2012.

[19] Antonius Jacobus Catherinus Schmeitz. *A Semi-Empirical Three-Dimensional Model of the Pneumatic Tyre Rolling over Arbitrarily Uneven Road Surfaces*. PhD thesis, TU Delft, Delft University of Technology, 2004.

[20] Cosin Scientific Software. *FTire - Flexible Structure Tire Model*.

[21] M. Yamakado, M. Abe, and Y. Kano. Fundamental study on ideal longitudinal control for improved dynamical handling characteristics. In *The Dynamics of Vehicles on Roads and Tracks: Proceedings of the 24th Symposium of the International Association for Vehicle System Dynamics (IAVSD 2015)*, Graz, Austria, August 2015. CRC Press.

[22] Peter Zegelaar. *The Dynamic Response of Tyres to Brake Torque Variations and Road Unevenesses*. PhD thesis, Delft University of Technology, 1998.

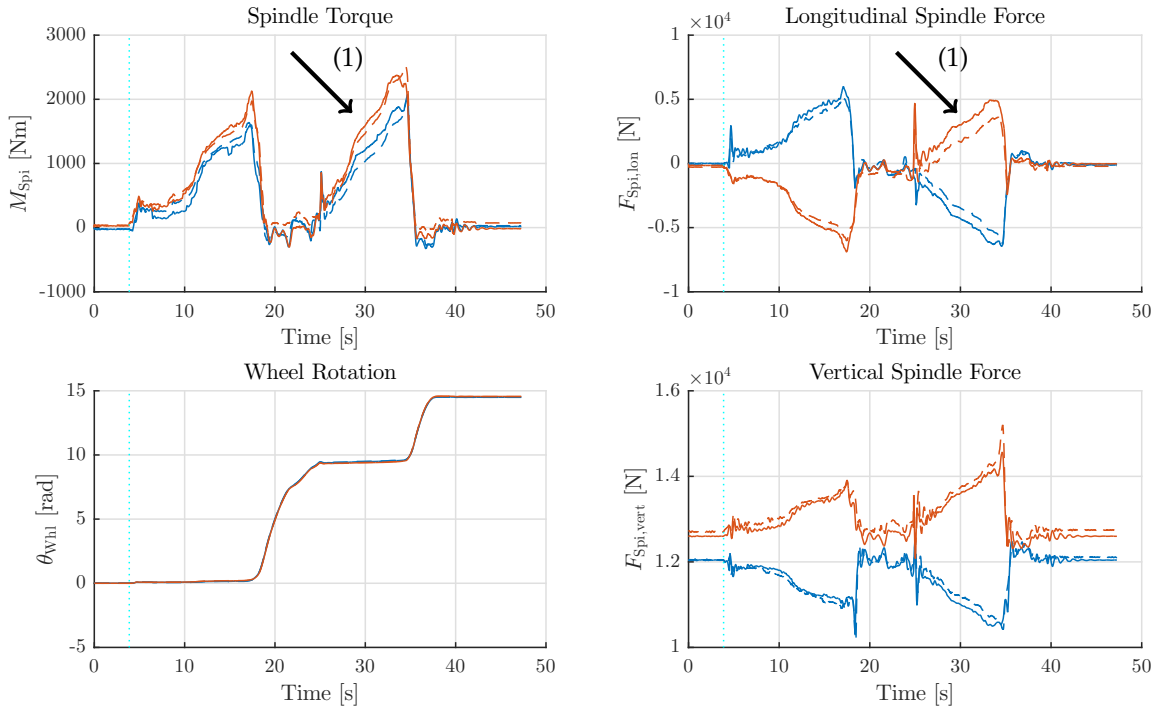

Figure 7: *Driving forward up a 14 cm step with both front (blue) and rear (red) axle. Simulation data is solid and measurement data is dashed.*

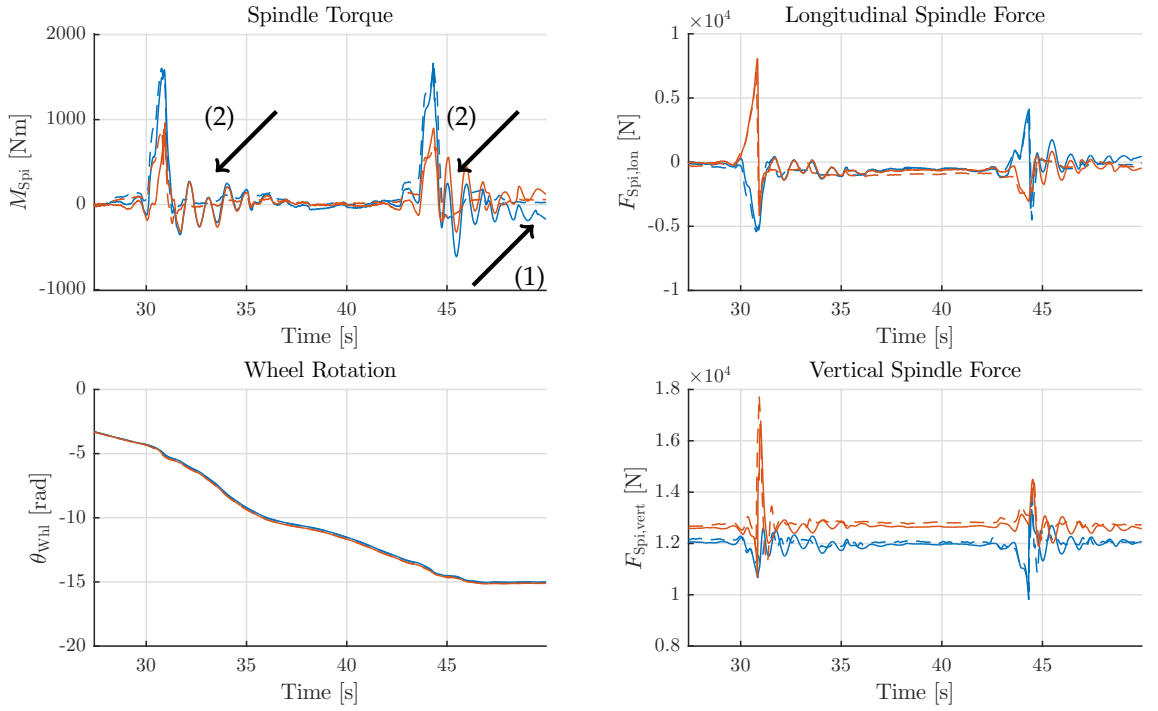

Figure 8: *Driving backward down a 14 cm step with both rear (red) and front (blue) axle. Simulation data is solid and measurement data is dashed.*

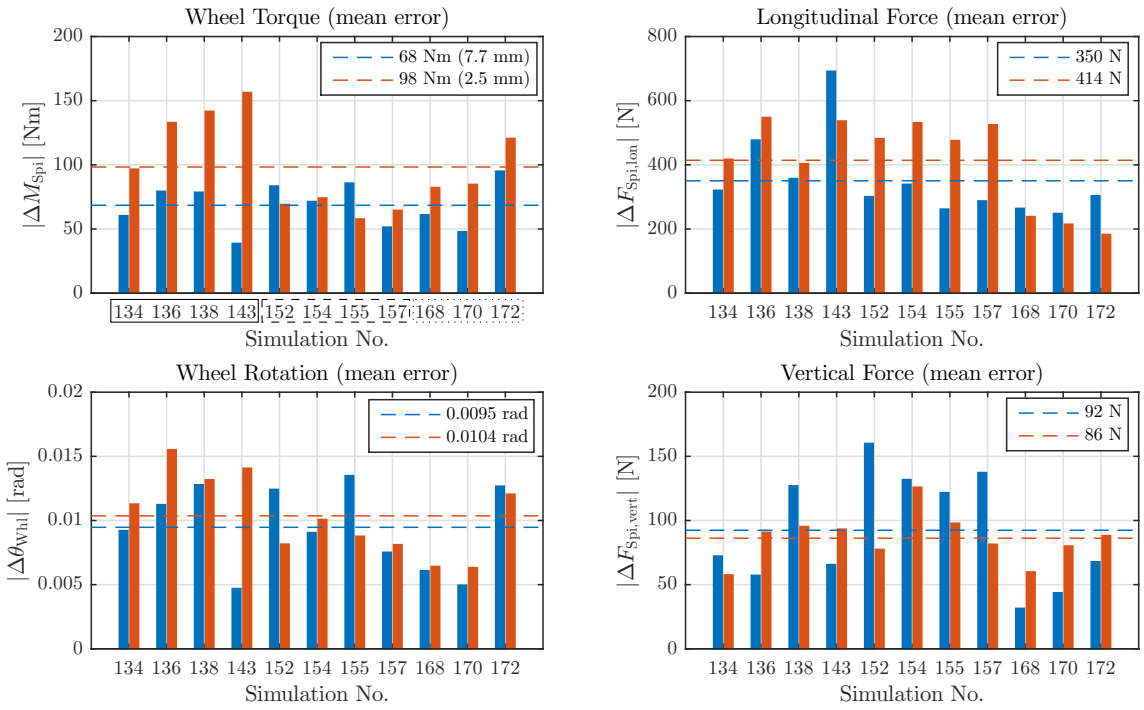

Figure 9: *Tire: Two Point Model. Mean simulation errors of driving up a step of 14 (solid group), 11 (dashed group) and 4 cm (dotted group) with the front wheel. The front wheel is blue, the rear wheel red. The horizontal lines indicate the mean of all simulations.*

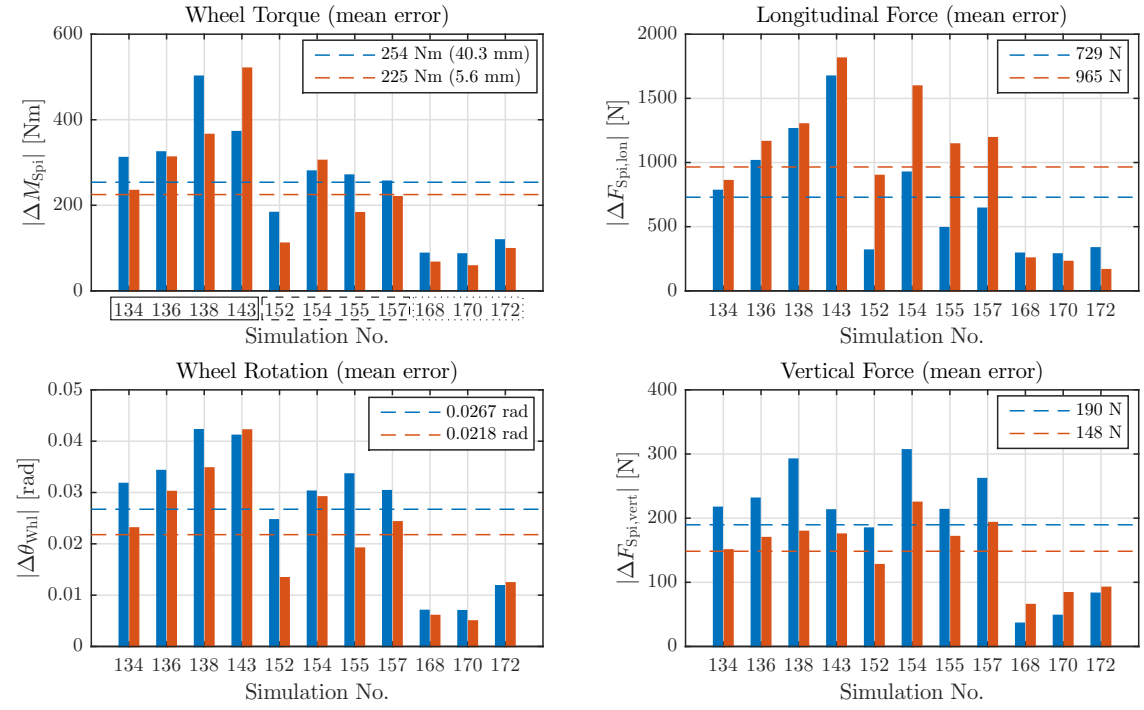

Figure 10: *Tire: Point Contact Model and Tandem Elliptical Cams. Mean simulation errors of driving up a step of 14 (solid group), 11 (dashed group) and 4 cm (dotted group) with the front wheel. The front wheel is blue, the rear wheel red. The horizontal lines indicate the mean of all simulations.*